Supporting Information

Coexistence Performance of Circularly Polarized Luminescence and Proton Conduction in Homochiral Cadmium(II)-Terbium(III) Complexes

Shui-Dong Zhu,[*a,b] Yu-Lin Zhou,[b] Yu Lei,[b] He-Rui Wen,[*a] Sui-Jun Liu,[a] Cai-Ming Liu,[c] Shi-Yong Zhang[b] and Ying-Bing Lu,[*b]

[a]School of Chemistry and Chemical Engineering, Jiangxi Provincial Key Laboratory of Functional Molecular Materials Chemistry, Jiangxi University of Science and Technology, Ganzhou 341000, Jiangxi Province, People's Republic of China.

[b]Jiangxi Key Laboratory of Function of Materials Chemistry, College of Chemistry and Chemical Engineering, Gannan Normal University, Ganzhou 341000, Jiangxi Province, People's Republic of China.

[c]Beijing National Laboratory for Molecular Sciences Center for Molecular Science, Institute of Chemistry, Chinese Academy of Sciences, Beijing 100190, People's Republic of China.

Corresponding authors. E-mail: zsd2002@sina.com (S.-D. Zhu), wenherui63@163.com (H.-R. Wen), ybluhm@163.com (Y.-B. Lu).

Table of Contents

Experimental Procedures

Materials and Instruments. Chemistry reagents and solvents were purchased from common commercial suppliers and were used without further purification. The synthestic methods of H_2L ligands were reported in the literature.[1] The FT-IR spectra were acquired in KBr disks on a Nicolet Magna 750 FT-IR spectrophotometer in the region of 4000−400 cm^{-1}. Powder X-ray diffraction (PXRD) patterns were collected on a Bruker ADVANCE D8 $\theta-2\theta$ diffractometer with Cu Kα radiation (λ = 1.54057 Å). Simulated PXRD patterns were obtained from the Mercury Version 1.4 software.[2] Thermogravimetry analysis (TGA) of ***R*-1** was measured on a NETZSCH STA2500 (TG/DTA) thermal analyser with a heating rates of 10 °C min^{-1} in nitrogen atmosphere in the temperature region of 25−800°C. The circular dichroism (CD) spectra were performed on a JASCO J-1500 spectropolarimeter. Circularly polarized luminescence (CPL) spectra of the ***R*/*S*-1** were recorded on JASCO CPL-300 instrument at room temperature in the solid state. Photoluminescence analyses were carried out on an Edinburgh FL S920 fluorescence spectrometer. Proton conductivity measurements of ***R*-1** were performed on a quasi-four-electrode AC impedance technique with a Solartron 1260 impedance/gain-phase analyzer to investigate the proton mobility at various temperatures and humidities. The microcrystalline samples were 0.80 mm and 2.50 mm for the diameter and thickness. Two sides of the pellet were connected to gold wires using gold paste. The proton conductivities of the samples were deduced from the Debye semicircle in the Nyquist plot. The conductivity was calculated by the equation $\sigma = L/(RS)$, σ ($S \cdot cm^{-1}$) means the conductivity, L (cm) is the thickness, R (Ω) is the resistance, and S (cm^2) is cross-sectional the area. The MCD spectra were measured using a JASCO J-810 magnetic circular dichroism spectrometer equipped with a permanent magnet (+1.0 T or −1.0 T).

Preparation of $[TbCd_2(RR/SS\text{-}L)_2(H_2O)_6](ClO_4)_3 \cdot 2H_2O$ (*R*-1 and *S*-1, H_2L = ((*RR/SS*)-cyclohexane-1,2-diylbis(azanediyl))-bis(methylene))-bis(2-methoxyphenol))): A mixture of *RR*-H_2L or *SS*-H_2L (36.8 mg, 0.1 mmol) and $Cd(ClO_4)_2 \cdot 6H_2O$ (42 mg, 0.1 mmol) in MeOH/$CHCl_3$ (10 mL/5 mL) was stirred for 20 minute. Then $Tb(ClO_4)_3 \cdot 6H_2O$ (40 mg, 0.1 mmol) was added and continuously stirred

for another 20 minutes. The resulting solution was filtered and left to evaporate at room temperature without disturbation. After several days, light yellow crystals were obtained and washed with $CHCl_3$. The yield is 50%−60% calculated based on rare earth salts. FT-IR peaks (KBr, cm^{-1}) for ***R*-1**: 3768(w), 3472(vs), 3420(vs), 2934(w), 1630(s), 1463(s), 1284(w), 1246(w), 1093(s), 952(w), 850(w), 722(s), 619(s), 479(w) ; for ***S*-1**: 3855(w), 3458(vs), 2947(w), 1630(s), 1463(s), 1297(s), 1106(w), 1079(s), 952(w), 836(w), 743(s), 632(s), 427(w) (Fig. S18).

Single-Crystal Structure Determination. Good-quality single crystal of ***R*-1** and ***S*-1** was used to collect the diffraction date on a Rigaku Mercury CCD diffractometer equipped with graphite-monochromated Mo-K*a* radiation (λ = 0.71073 Å). The raw intensity dates were reduced and collected through the SAINT software.[3] The olex2 program and the ShelXL-2015 refinement package were utilized to solve the two structures.[4-5] The difference Fourier map was employed for locating non-hydrogen atoms. Hydrogen atoms were placed in their calculated positions geometrically and refined according to the riding model. Higher space group was absent using the PLATON software from the IUCr website (http://www.iucr.org/).[6] Pertinent crystal data, structure refinement results, selected bond lengths and bond angles of ***S*-1** and ***R*-1** were all displayed in Table S1 and Table S2 in the ESI. CCDC-2168379 for ***R*-1** and CCDC-2168380 for ***S*-1** contains the supplementary crystallographic data for this work. These structure data that can be obtained free of charge were reserved in the Cambridge Crystallographic Data Centre in CIF format.

Table S1. Crystal data for ***R*-1** and ***S*-1**.

	***R*-1**	***S*-1**
Formula	$C_{44}H_{72}Cd_2Cl_3N_4O_{28}Tb$	$C_{44}H_{72}Cd_2Cl_3N_4O_{28}Tb$
Fw	1595.12	1595.12
Temp (K)	293(2)	296(2)
Crystal system	Orthorhombic	Orthorhombic
Space group	$C222_1$	$C222_1$
a, Å	16.9637(6)	16.8994(10)
b, Å	19.1882(7)	19.1280(10)
c, Å	18.3579(8)	18.3001(9)
b, (deg)	90	90
V, Å^3	5975.5(4)	5915.5(6)
Z	4	4
D_c, g/cm^3	1.773	1.791
m (mm^{-1})	2.097	2.119
F (000)	3200	3200
Reflns collected	9486	33834
Independent reflns	6150	5486
R_{int}	0.0239	0.0863
Theta range, °	3.39–27.50	3.08–25.49
Params/restraints/data	379 / 155 / 6150	379 / 38 / 5486
R_1 [$I > 2\sigma(I)$]	0.0494	0.0670
wR_2 (all data)	0.1195	0.1361
GOF on F^2	1.054	1.088
ρ_{max}/ρ_{min}, e Å^{-3}	2.56 / –0.95	1.27 / –1.72

$^a R1 = ||F_o|-|F_c||/|F_o|$; $^b wR2 = [w(F_o^2-F_c^2)^2]/[w(F_o^2)^2]^{1/2}$

Table S2. Selected bond lengths (Å) and angles (°) for ***R*-1** and ***S*-1**.

Complex ***R*-1** (bond)	lengths (Å)	(angle)	angles (°)
Tb(1)-O(2)	2.323(5)	O(2)-Tb(1)-O(2)#1	86.2(3)
Tb(1)-O(2)#1	2.323(5)	O(3)-Tb(1)-O(2)	73.34(17)
Tb(1)-O(3)	2.260(5)	O(3)-Tb(1)-O(2)#1	151.69(16)
Tb(1)-O(3)#1	2.260(5)	O(2)-Tb(1)-O(1W)#1	88.76(19)
Tb(1)-O(1W)#1	2.395(6)	O(2W)-Cd(2)-O(2)	85.2(3)
Tb(1)-O(1W)	2.395(6)	O(2W)-Cd(2)-N(2)	119.4(3)
Tb(1)-O(4)	2.621(5)	O(3)-Cd(2)-N(1)	110.12(19)
Tb(1)-O(4)#1	3.621(5)	O(2W)-Cd(2)-N(1)	157.3(3)
Cd(2)-O(2W)	2.271(8)	N(1)-Cd(2)-O(2)	86.51(19)
Cd(2)-N(2)	2.336(6)	N(1)-Cd(2)-N(2)	78.0(2)
Cd(2)-N(1)	2.288(6)		
Cd(2)-O(2)	2.340(5)		
Complex ***S*-1** (bond)	lengths (Å)	(angle)	angles (°)
Tb(1)-O(1W)#1	2.383(6)	O(3)-Tb(1)-O(3)#1	131.8(2)
Tb(1)-O(2)#1	2.317(5)	O(3)-Tb(1)-O(2)	75.51(17)
Tb(1)-O(3)#1	2.261(5)	O(3)-Tb(1)-O(2)#1	151.72(17)
Tb(1)-O(4)#1	2.611(5)	O(1W)#1-Tb(1)-O(1W)	153.6(3)
Tb(1)-O(1W)	2.383(6)	O(2W)-Cd(2)-O(3)	161.8(2)
Tb(1)-O(2)	2.317(5)	O(2W)-Cd(2)-N(1)	87.8(3)
Tb(1)-O(3)	2.261(5)	O(3)-Cd(2)-N(1)	110.4(2)
Tb(1)-O(4)	2.610(5)	O(2W)-Cd(2)-N(2)	101.9(3)
Cd(2)-O(3)	2.289(5)	O(3)-Cd(2)-N(2)	83.45(19)
Cd(2)-N(1)	2.273(6)	N(1)-Cd(2)-N(2)	78.5(2)
Cd(2)-N(2)	2.335(6)		
Cd(2)-O(2)	2.330(5)		

[a]Symmetry Codes for ***R*-1**: #1 *x*, –*y*+1, –*z* ; For ***S*-1**: #1 *x*, –*y*, –*z*, #2 –*x*+1, *y*, –*z*+1/2.

By using *SHAPE* 2.1 software[7], the coordination polyhedrons of Tb1(III) ion and Cd1(II) ion can be described as a distorted square antiprism and a distorted octahedron, respectively (Fig. S1, Tables S3), with a continuous shape measure (CSHM) values of 5.893 for Tb1(III) and 5.400 for Cd1(II), respectively (Table S3). The two square bases of the square antiprism are formed by the atoms (O2, O3, O4 and O1W) and (O2A, O3A, O4A and O1WA) respectively, with the Tb1 atom located near the centre of the square antiprism. In the trimer of ***R*-1**, the distance between Cd1 and Tb1 is 3.6862(1) Å.

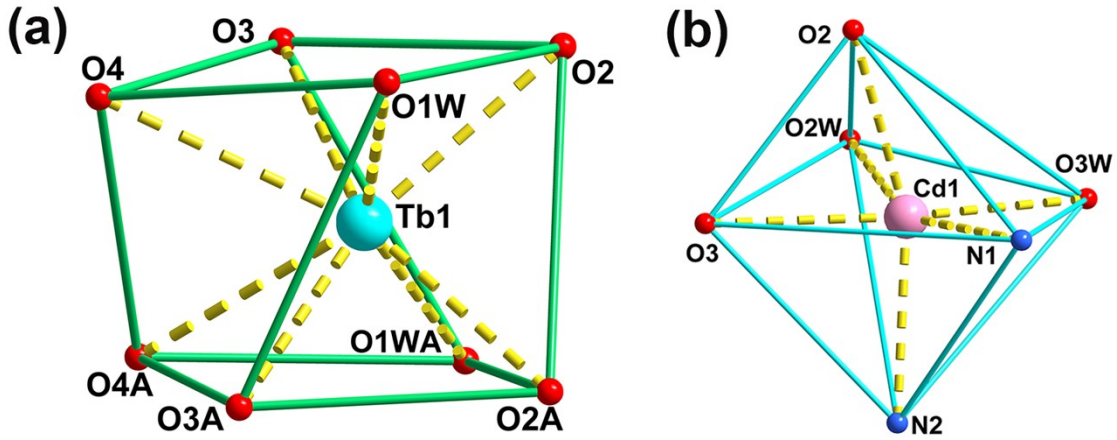

Fig. S1 (a) The cooordination polyhedron around the Tb1 of ***R*-1**; (b) The cooedination environment around the Cd1 of ***R*-1**; The H and C atoms are omitted for clarity.

Table S3 Summary of SHAPE analysis for ***R*-1**.

Metal	label	shape	symmetry	Distortion(τ)
Cd	HP-6	Hexagon	D_{6h}	33.565
	PPY-6	Pentagonal pyramid	C_{5v}	15.868
	OC-6	**Octahedron**	**O_h**	**5.400**
	TPR-6	Trigonal prism	D_{3h}	5.538
	JPPY-6	Johnson pentagonal pyramid J2	C_{5v}	19.359
Tb	OP-8	Octagon	D_{8h}	26.901
	HPY-8	Heptagonal pyramid	C_{7v}	16.938
	HBPY-8	Hexagonal bipyramid	D_{6h}	15.754
	CU-8	Pentagonal prism	O_h	15.810
	SAPR-8	**Square antiprism**	**D_{4d}**	**5.893**
	TDD-8	Square antiprism	D_{2d}	5.952
	JGBF-8	Johnson gyrobifastigium J26	D_{2d}	13.775
	JETBPY-8	Johnson elongated triangular bipyramid J14	D_{3h}	19.768
	JBTPR-8	Biaugmented trigonal prism J50	C_{2v}	6.275
	BTPR-8	Biaugmented trigonal prism	C_{2v}	6.098
	JSD-8	Snub diphenoid J84	D_{2d}	8.264
	TT-8	Triakis tetrahedron	T_d	16.196
	ETBPY-8	Elongated trigonal bipyramid	D_{3h}	16.229

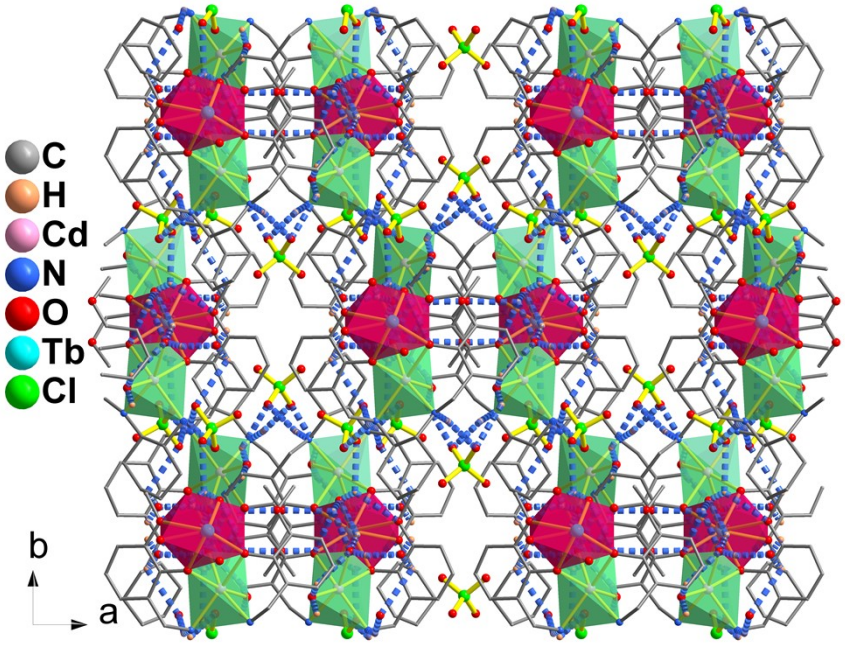

Fig. S2 The 3D supramolecular network of ***R*-1** constructed by hydrogen bond interactions (blue dashed lines).

Table S4 H-bonding lengths and angles for ***R*-1**.

D-H…A	d(H…A)(Å)	d(D…A)(Å)	<DHA(Å)
N(1)–H(1)…O(9)	2.28	3.243(10)	170
N(2)–H(2)…O(5)	2.28	3.200(13)	157
N(2)–H(2)….O(8)	2.34	3.209(16)	147
O1W–H1WA…O(6)	2.34	2.840(12)	116
O2W–H2WB…O4W	1.77	2.687(15)	164
O3W–H3WB…O(9)	2.44	3.132(13)	136
O4W–H4WA…O(8)	3.78	2.958（1）	16
O4W–H4WB…O(8)	2.62	2.958（1）	105
Intra O1W–H1WA…O(4)	2.54	2.920(8)	108
Intra O1W–H1WB…O(1)	2.38	2.698(8)	101
Intra O1W–H1WB…O2W	2.38	3.089(9)	138
Intra O2W–H2WA…O1W	2.33	3.089(9)	138
Intra O3W–H3WA…O2W	2.48	2.808(12)	103

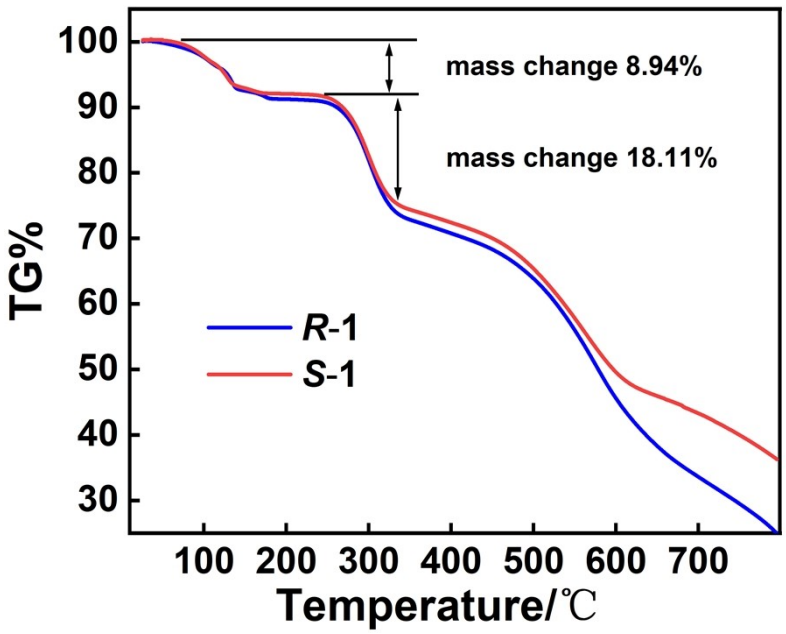

Fig. S3 The TGA plots of ***R*-1** and ***S*-1**.

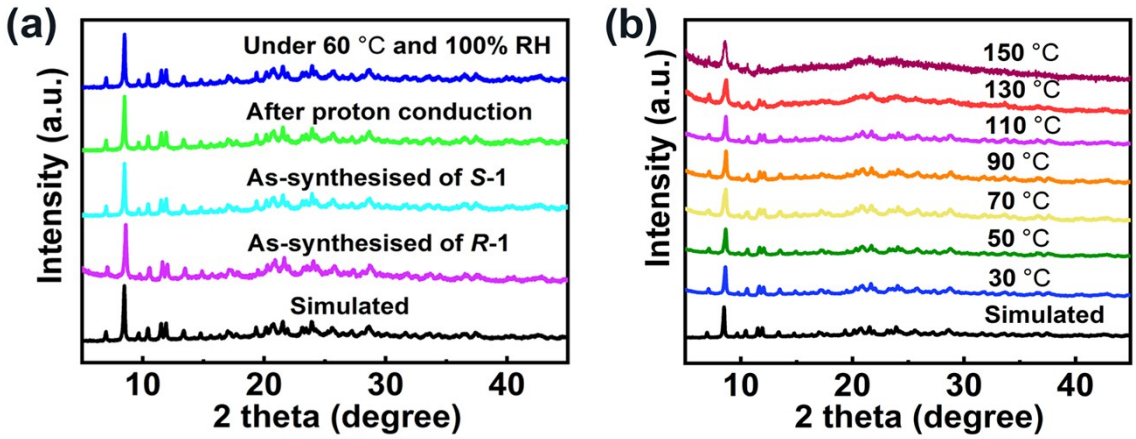

Fig. S4 (a) PXRD patterns of the simulated one, as-synthesized ***R*-1** and ***S*-1**, after proton conduction and exposing under 60 °C and 100% RH conditions for 24 hours of ***R*-1**; (b) PXRD patterns of ***R*-1** after heated at different temperature for 24 hours.

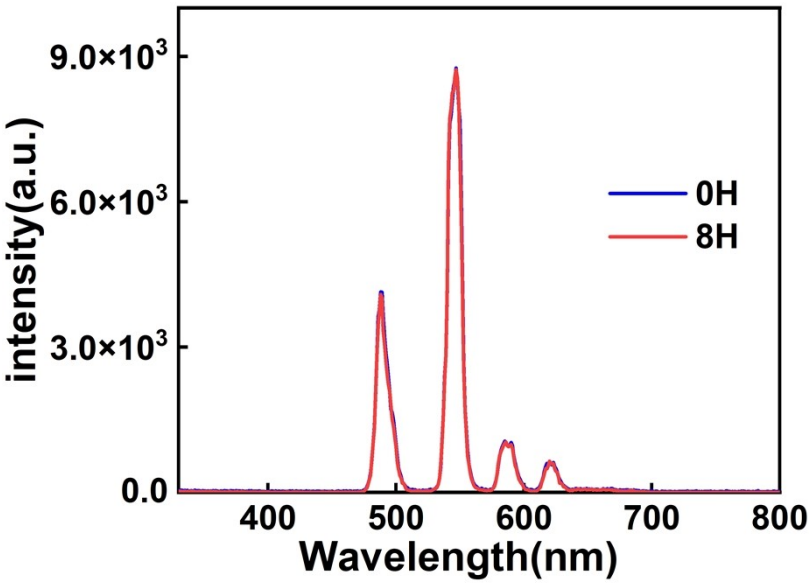

Fig. S5 Comparison of emission spectra of ***R*-1** in methanol solution after being placed for 0 h and 8 h.

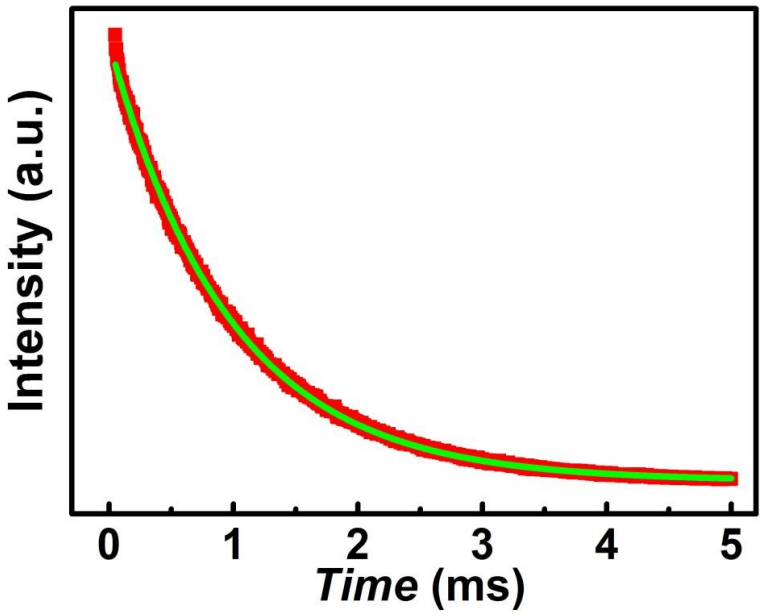

Fig. S6 Decay curves of ***R*-1** at room temperature.

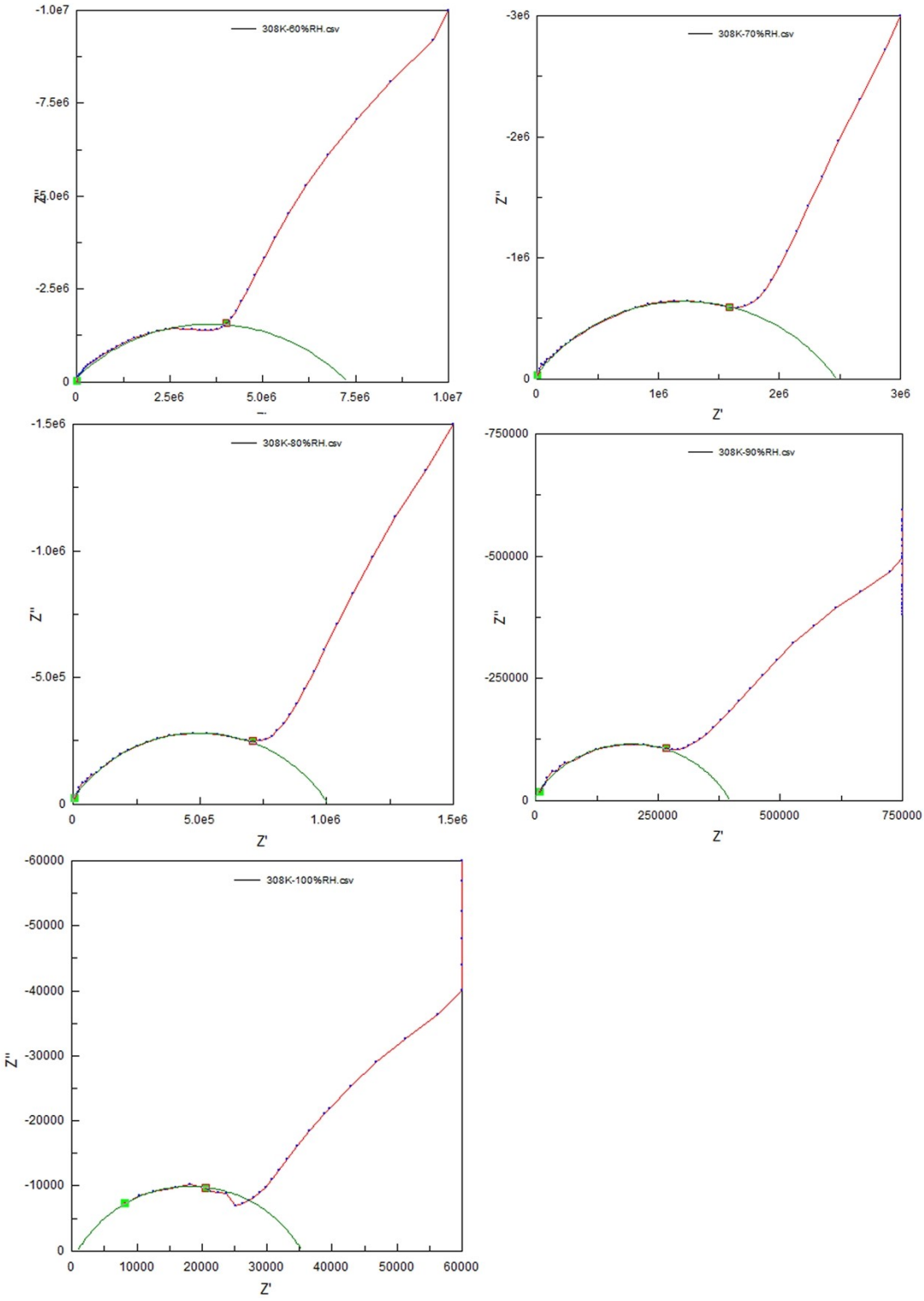

Fig. S7 The best-fit result of Nyquist plot for ***R*-1** at 303K under different RH levels.

Table S5 The proton conductivity of ***R*-1** at 303K under variable relative humidity (RH).

RH / %	R/Ω	□ □□σ / S cm^{-1}
60	7.41× 10^6	2.15 × 10^{-7}
70	2.50× 10^6	6.37 × 10^{-7}
80	1.02× 10^6	1.56 × 10^{-6}
90	4.05×10^5	3.93 × 10^{-6}
100	3.45× 10^4	4.61 × 10^{-5}

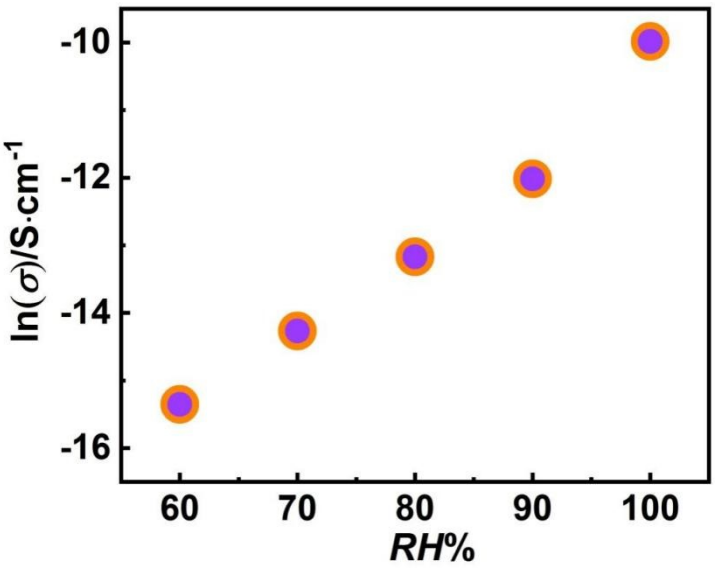

Fig. S8 Plot of proton conductivity for ***R*-1** vs. RH at 303K.

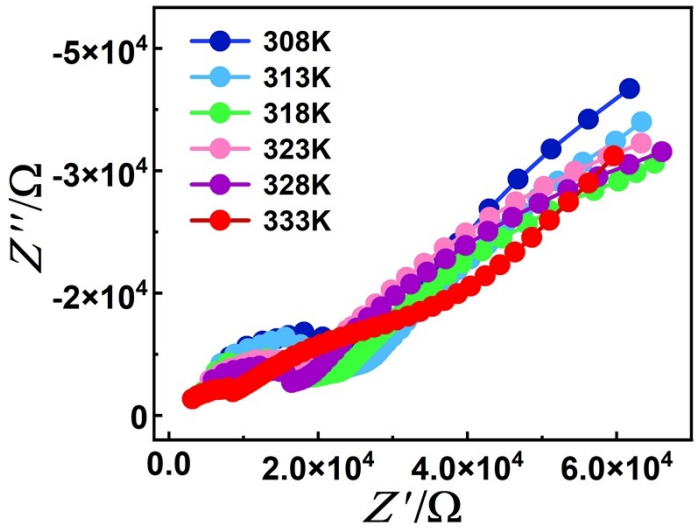

Fig. S9 The temperature-dependent impedance diagrams of ***R*-1** at 100% RH.

Table S6 The proton conductivity of ***R*-1** at 100% RH under variable temperatures (K).

Temperature / K	R/Ω	□□ σ / S cm^{-1}
308	3.45× 10^4	4.61 × 10^{-5}
313	2.82×10^4	5.64 × 10^{-5}
318	2.26×10^4	7.05 × 10^{-5}
323	1.90×10^4	8.36 × 10^{-5}
328	1.47×10^4	1.08× 10^{-4}
333	1.36×10^4	1.17 × 10^{-4}

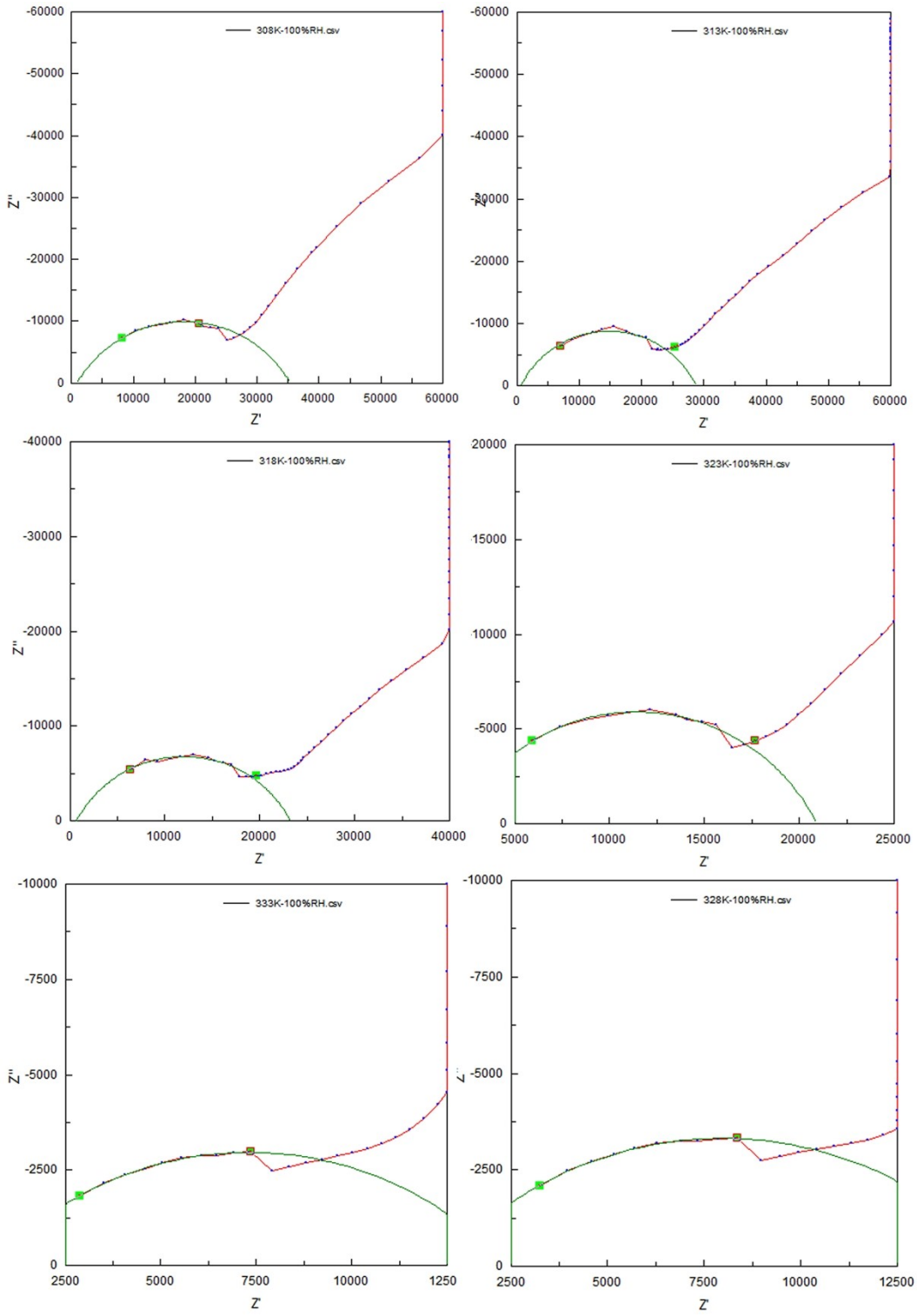

Fig. S10 The best-fit result of Nyquist plot for ***R*-1** at different temperatures under 100% RH

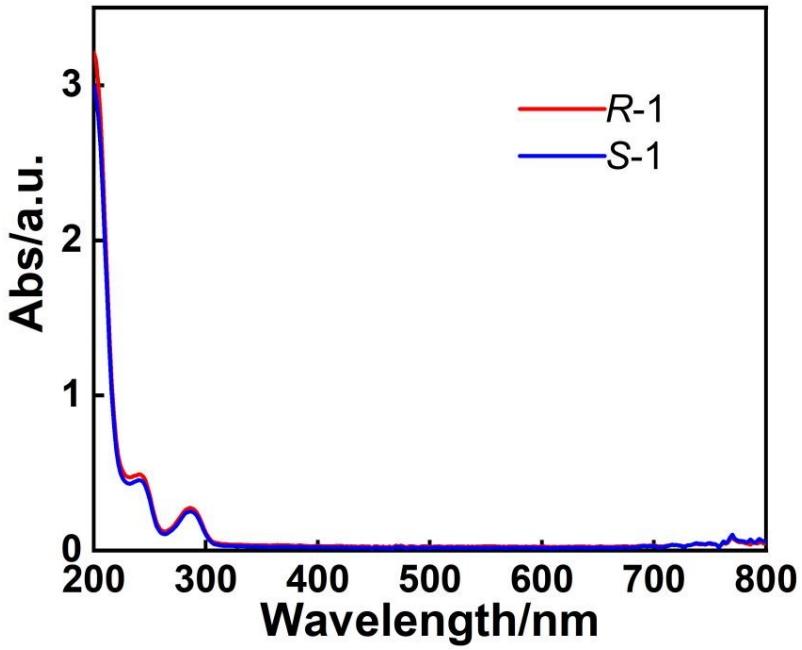

Fig. S11 UV spectra of ***R*-1** and ***S*-1** in CH_3OH

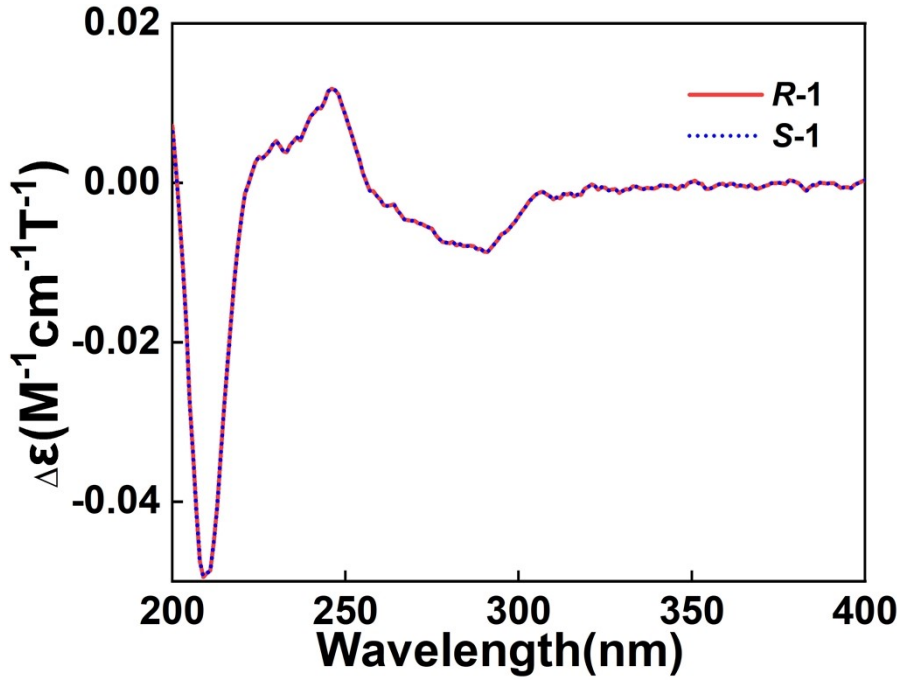

Fig. S12 MCD spectra of enantiomers ***R*-1** and ***S*-1** in a CH_3OH solution (c = 0.2 g L^{-1}) at room temperature.

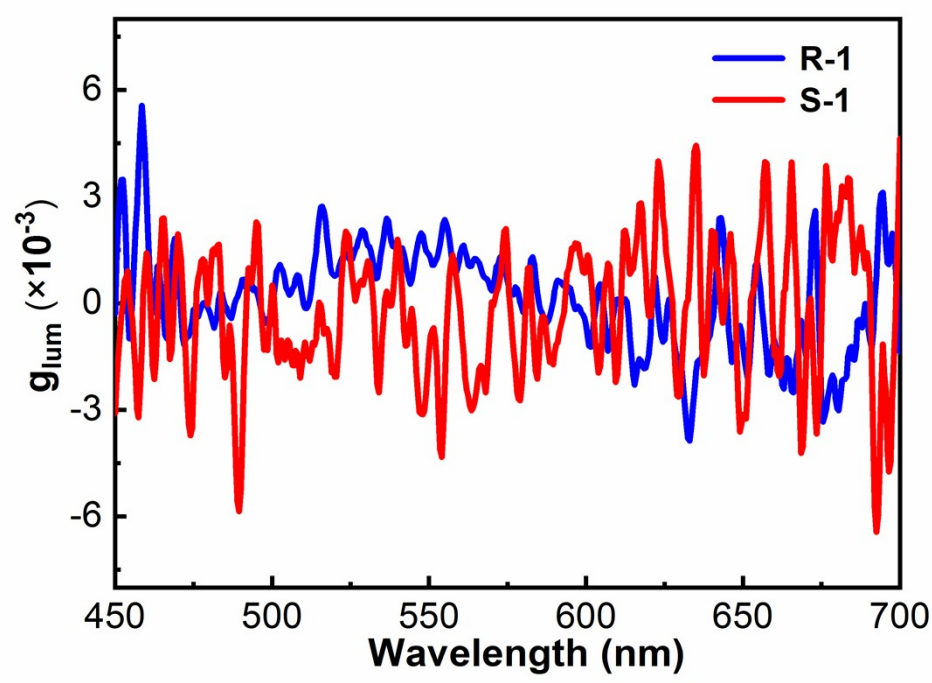

Fig. S13 Corresponding g_{lum} values (CPL) of ***R*-1** and ***S*-1** in CH_3OH.

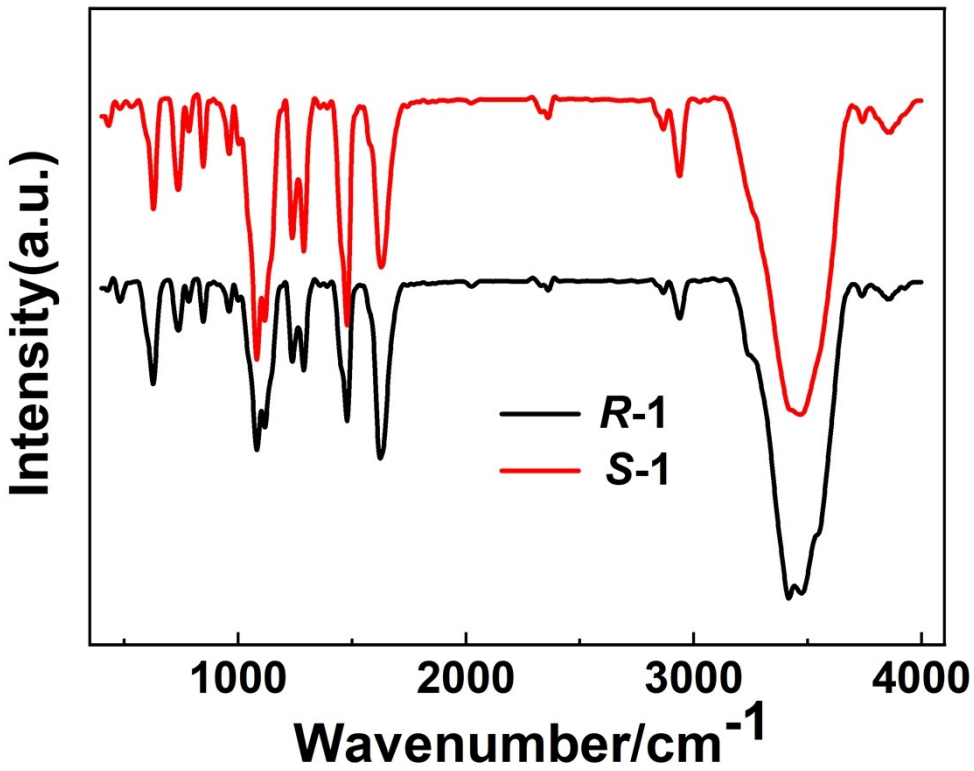

Fig. S14 IR spectrum of ***R*-1** and ***S*-1**.

References

1. E. C. Constable, G. D. Zhang, G. D. Housecroft, M. Neuburger, S. Schaffner and W. D.Woggon, *New. J. Chem*. 2009, **33**, 1064−1069.
2. C. F. Macrae, P. R. Edgington, P. McCabe, E. Pidcock, G. P. Shields, R. Taylor, M. Towler and J. van de Streek, *J. Appl. Crystallogr.* 2006, **39**, 453−457.
3. G. M. Sheldrick, SADABS, Program for Empirical Absorption Correction of Area Detector Data; *University of Göttingen: Germany*, 1996.
4. *CrystalClear, version 1.35, Software User's Guide for the Rigaku R-Axis, and Mercury and Jupiter CCD Automated X−ray Imaging System*; Rigaku Molecular Structure Corporation: Utah, 2002.
5. O. V. Dolomanov, L. J. Bourhis, R. J. Gildea, J. A. K. Howard and H. Puschmann, OLEX2: A Complete Structure Solution, Refinement and Analysis Program, *J. Appl. Crystallogr.* 2009, **42**, 339–341.
6. A. L. Spek, Structure validation in chemical crystallography, *Acta Cryst.* **2009**, **D65**, 148–155.
7. M. Llunell, D. Casanova, J. Cirera, P. Alemany, S. Alvarez, *SHAPE*; version 2.1; Electronic Structure Group, Universitat de Barcelona, Spain, 2013.